On the equivalence of the Trefftz method and method of fundamental solutions for Laplace and biharmonic equations

J.T. Chen [a,*], C.S. Wu [a], Y.T. Lee [a], K.H. Chen [b]

[a] *Department of Harbour and River Engineering, National Taiwan Ocean University, Keelung 20224, Taiwan*
[b] *Department of Information Management, Toko University, Chia-Yi 631, Taiwan*

Abstract

In this paper, it is proved that the two approaches, known in the literature as the method of fundamental solutions (MFS) and the Trefftz method, are mathematically equivalent in spite of their essentially minor and apparent differences in formulation. In deriving the equivalence of the Trefftz method and the MFS for the Laplace and biharmonic problems, it is interesting to find that the complete set in the Trefftz method for the Laplace and biharmonic problems are embedded in the degenerate kernels of the MFS. The degenerate scale appears using the MFS when the geometrical matrix is singular. The occurring mechanism of the degenerate scale in the MFS is also studied by using circulant. The comparison of accuracy and efficiency of the two methods was addressed.
© 2007 Elsevier Ltd. All rights reserved.

1. Introduction

In 1926, Trefftz presented the Trefftz method for solving boundary value problems by superimposing the functions satisfying the governing equation, although various versions of Trefftz method, e.g. direct formulation and indirect formulations have been developed [13]. The unknown coefficients are determined by matching the boundary condition. Many applications to the Laplace equation [1], the Helmholtz equation [5], the Navier equation [6,7] and the biharmonic equation [8] were done. Not until recent years has the ill-posed nature in the method been noticed [2].

In theory, it is well known that the MFS can solve potential problems when a fundamental solution is known. This method was proposed by Kupradze [14] in Russia. Extensive applications in solving a broad range of problems such as potential problems [1,5,12], elasticity [7,14] acoustics [5] and biharmonic problems (plate) [8–11] have been studied. The MFS can be reviewed as an indirect boundary element method with a concentrated source instead of distribution. The initial idea is to approximate the solution through a linear combination of fundamental solutions with sources located outside the domain of the problem. Moreover, it has certain advantages over BEM, e.g. no singularity and no boundary integrals are required. However, ill-posed behaviour is inherent in the regular formulation.

---

* Corresponding author. Tel.: +886 2 24622192x6140.
E-mail address: jtchen@mail.ntou.edu.tw (J.T. Chen).

Nomenclature

a	radius of the circular problem
a_0	Fourier coefficient for boundary density
a_n	Fourier coefficient for boundary density
B	boundary
$[C]$	Circulant matrix
c_j	Coefficient of the MFS
b_n	Fourier coefficient for boundary density
D	flexural rigidity
$[K^I]$	mapping matrix of interior problem
$[K^E]$	mapping matrix of exterior problem
$L(s, x)$	kernel function
N_T	the number of T-complete function
N_M	the number of the source point in MFS
n	normal vector
n_s	normal vector at the source point s
n_x	normal vector at the field point x
p_n	Fourier coefficient for boundary density
q_n	Fourier coefficient for boundary density
r	distance between the source point s and the field point x, $r = |x - s|$
s	position vector of source point
t	tangential vector
$t(s)$	tangential vector at the source point s
$t(x)$	tangential vector at the field point x
$\bar{u}$	Dirichlet-type boundary condition
$u(x)$	displacement
$u_j(x)$	T-complete set of Trefftz method
$U(s, x)$	kernel function of MFS
$[U]$	influence matrix of the kernel function $U(s, x)$
w_j	coefficient of the Trefftz method
x	position vector of the field point
$\theta(x)$	slope
(R, θ)	polor coordinates of s
(ρ, ϕ)	polor coordinates of x
∇^2	Laplace operator
∇^4	biharmonic operator
Ω	domain
Ω^c	complementary domain

Although both have a long history, the link between the Trefftz method and the MFS was not detailed discussion in the literature to the authors' best knowledge. A similar case to link the DRBEM and the method of particular integral was done by Polyzos et al. [15].

In this paper, we solve the interior and exterior Laplace problems with a circular boundary and prove the mathematical equivalence between the Trefftz method and the MFS. Three mathematical tools are utilized. One is the degenerate kernel [3] for the expansion of the closed-form fundamental solution, another is the Fourier series expansion for the boundary density and the other is the circulant which is employed to study the degenerate scale [4] in the MFS. The ill-posed behaviour of the MFS is also addressed. The efficiency of the Trefftz method and MFS is compared with the same number of unknowns. Also, the error analysis of MFS and the Trefftz method is discussed. Based on the successful experiences of the Laplace equation, we extend it to the biharmonic equation and discuss

the behaviour of the rank-deficiency in the mapping matrix when deriving the equivalence of the Trefftz method and MFS. Finally, the occurring mechanism of the degenerate scales will be examined.

2. On the independent bases in the Trefftz method and the MFS

2.1. Trefftz method

In the Trefftz method, the field solution $u(x)$ is superimposed by the complete functions, $u_j(x)$ as follows:

$$u(x) = \sum_{j=1}^{N_T} \omega_j u_j(x), \tag{1}$$

where N_T is the number of complete functions, ω_j is the jth unknown coefficient to be determined by matching the boundary condition, $u_j(x)$ is the jth complete function which satisfies the governing equation.

2.2. Method of fundamental solutions (MFS)

In the MFS, the field solution $u(x)$ is superimposed by the fundamental solution, $U(x, s)$, as follows:

$$u(x) = \sum_{j=1}^{N_M} c_j U(x, s_j), \quad s_j \in \Omega^e \tag{2}$$

where N_M is the number of source points in the MFS, c_j is the jth unknown coefficient, s and x are the source point and collocation point, respectively, Ω^e is the complementary domain and $U(x, s)$ is the corresponding fundamental solution.

2.3. On the complete set of the Trefftz method and the MFS using the degenerate kernel

By expanding the fundamental solution in the MFS, we have the general form as shown in Fig. 1(a) and (b).

$$U(x, s) = \begin{cases} U^I(x, s) = \displaystyle\sum_{j=1}^{\infty} A_j(x)B_j(s), & |x| < |s|, \\ U^E(x, s) = \displaystyle\sum_{j=1}^{\infty} A_j(s)B_j(x), & |x| > |s|, \end{cases} \tag{3}$$

where the superscripts of "I" and "E" denote the interior and exterior domains, respectively. It is interesting to find that all the complete sets, $u_j(x)$, in the Trefftz method are embedded in $A_j(x)$ and $B_j(x)$ for the interior and exterior problems. To demonstrate this point, we summarize the complete sets in the Trefftz method and degenerate kernels of the MFS for the Laplace and biharmonic equations in Tables 1 and 2. The tables point out that the Trefftz bases can be obtained through the degenerate kernel.

3. Connection between the Trefftz method and the MFS for interior and exterior Laplace problems

Consider the two-dimensional Laplace problem with a circular domain (interior problem) or a circular hole (exterior problem) of radius a as shown in Figs. 2(a) and 2(b). The governing equation of the boundary value problem is the Laplace equation:

$$\nabla^2 u(x) = 0, \quad x \in \Omega, \tag{4}$$

where Ω is the domain of interest, ∇^2 denotes the Laplacian operator and $u(x)$ is the potential function. The boundary condition is given by the Dirichlet type

$$u(x) = \overline{u}, \quad x \in B. \tag{5}$$

Table 1
T-complete functions of the Trefftz method and degenerate kernels of the MFS for the Laplace equation

| | | Method of fundamental solution (MFS) | | Trefftz method | |
		Fundamental solution	Degenerate kernel	Interior basis	Exterior basis
Basis functions and degenerate kernels	1-D	$\frac{r}{2}$	$U(x,s) = \begin{cases} \frac{1}{2}(x-s), & x>s \\ \frac{1}{2}(s-x), & x<s \end{cases}$	$1, x$	$1, x$
	2-D	$\ln(r)$	$U(x,s) = \begin{cases} U^i(x,s) = \ln R - \sum_{m=1}^{\infty}\frac{1}{m}\left(\frac{\rho}{R}\right)^m \cos(m(\phi-\theta)), & \rho < R \\ U^e(x,s) = \ln \rho - \sum_{m=1}^{\infty}\frac{1}{m}\left(\frac{R}{\rho}\right)^m \cos(m(\phi-\theta)), & \rho > R \end{cases}$	$1,$ $\rho^m \cos(m\theta),$ $\rho^m \sin(m\theta)$	$\ln(\rho),$ $\rho^{-m}\cos m\theta$ $\rho^{-m}\sin m\theta$
	3-D	$\frac{-1}{r}$	$U(x,s) = \begin{cases} U^I(x,s) = \frac{-1}{R} - \sum_{n=1}^{\infty}\sum_{m=0}^{\infty} P_n^m(\cos\theta)]P_n^m(\cos\phi)]\frac{\rho^n}{R^{n+1}}\frac{(n-m)!}{(n+m)!} \\ \qquad\times \cos[m(\phi-\theta)], \quad R > \rho \\ U^E(x,s) = \frac{-1}{\rho} - \sum_{n=1}^{\infty}\sum_{m=0}^{\infty} P_n^m(\cos\theta)]P_n^m(\cos\phi)]\frac{\frac{R^n}{\rho^{n+1}}(n+m)!}{(n-m)!} \\ \qquad\times \cos[m(\phi-\theta)], \quad R < \rho \end{cases}$	$\rho^n P_n^m(\cos\theta)\cos(m\phi)$ $\rho^n P_n^m(\cos\theta)\sin(m\phi)$	$\rho^{-(n+1)}P_n^m(\cos\theta)\cos(m\phi)$ $\rho^{-(n+1)}P_n^m(\cos\theta)\sin(m\phi)$
The basis function which satisfies the equation	1-D		$\frac{\partial^2}{\partial x^2}U(x,s) = \delta(x-s)$	$\frac{d^2}{dx^2}u(x) = 0$	
	2-D		$\nabla^2 U(x,s) = 2\pi\delta(x-s)$	$\nabla^2 u(\rho,\phi) = 0$	
	3-D		$\nabla^2 U(x,s) = 4\pi\delta(x-s)$	$\nabla^2 u(\rho,\theta,\phi) = 0$	

where $m = 0, 1, 2, 3, \ldots$ and $n = 0, 1, 2, 3, \ldots$.

Table 2
T-complete functions of the Trefftz method and degenerate kernels of the MFS for the biharmonic equation

| | Method of fundamental solution (MFS) | | Trefftz method | |
	Fundamental solution	Degenerate kernel	Interior basis	Exterior basis
Basis function and degenerate kernels	1-D $\frac{1}{12}r^3$	$U(s,x) = \begin{cases} \frac{1}{12}(x^3 - 3x^2 s + 3xs^2 - s^3), & x > s \\ \frac{1}{12}(s^3 - 3s^2 x + 3sx^2 - x^3), & x < s \end{cases}$	$1, x, x^2, x^3$	$1, x, x^2, x^3$
	2-D $r^2 \ln(r)$	$U(s,x) = \begin{cases} U^I(s,x) = \rho^2(1 + \ln R) + R^2 \ln R - R\rho(1 + 2\ln R)\cos(\theta - \phi) \\ \quad - \sum_{m=1}^{\infty} \frac{1}{m(m+1)} \frac{\rho^{m+2}}{R^m} \cos[m(\theta - \phi)] \\ \quad + \sum_{m=2}^{\infty} \frac{1}{m(m-1)} \frac{\rho^m}{R^{m-2}} \cos[m(\theta - \phi)], \; R > \rho \\ U^E(s,x) = R^2(1 + \ln \rho) + \rho^2 \ln \rho - \rho R(1 + 2\ln \rho)\cos(\theta - \phi) \\ \quad - \sum_{m=1}^{\infty} \frac{1}{m(m+1)} \frac{R^{m+2}}{\rho^m} \cos[m(\theta - \phi)] \\ \quad + \sum_{m=2}^{\infty} \frac{1}{m(m-1)} \frac{R^m}{\rho^{m-2}} \cos[m(\theta - \phi)], \; \rho > R \end{cases}$	$1, \rho^2,$ $\rho^m \cos(m\phi), \rho^m \sin(m\phi)$ $\rho^{m+2} \cos(m\phi), \rho^{m+2} \sin(m\phi)$	$\ln(\rho), \rho^2 \ln(\rho)$ $\rho^{-m} \cos(m\phi), \rho^{-m} \sin(m\phi)$ $\rho^{2-m} \cos(m\phi), \rho^{2-m} \sin(m\phi)$
The basis function which satisfy the equation	1-D	$\frac{\partial^4 U(x,s)}{\partial x^4} = \delta(x - s)$	$\frac{d^4 u(x)}{dx^4} = 0$	
	2-D	$\nabla^4 U(x,s) = 8\pi \delta(x - s)$	$\nabla^4 u(\rho, \phi) = 0$	

Where $m = 0, 1, 2, 3, \ldots$.

x: variable   s: fixed
(a): closed form
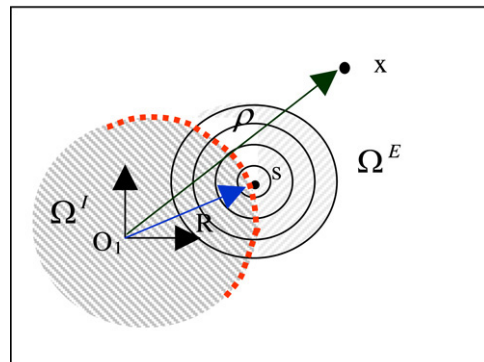
(b): series form (Degenerate kernel)

Fig. 1. Fundamental solution: (a) closed form; (b) series form (Degenerate kernel).
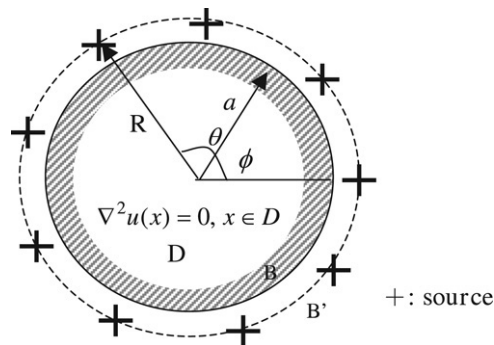
Fig. 2(a). Definition sketch for the interior Laplace equation with the circular domain using the polar coordinate.

By using the Fourier series expansion, the boundary condition can be expressed as

$$u(a, \phi) = \overline{a}_0 + \sum_{n=1}^{N} \overline{a}_n \cos(n\phi) + \sum_{n=1}^{N} \overline{b}_n \sin(n\phi) \tag{6}$$

where $\overline{a}_0$, $\overline{a}_n$ and $\overline{b}_n$ are the Fourier coefficients with respect to the Fourier bases, $\cos(n\phi)$ and $\sin(n\phi)$, and ϕ is the angle along the circular boundary.
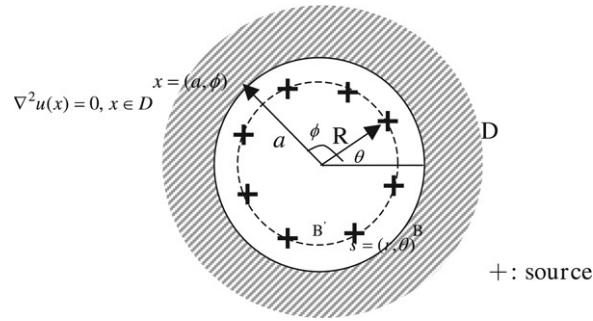
Fig. 2(b). Definition sketch for the exterior Laplace problem with the circular hole using the polar coordinate.

3.1. Trefftz method

In the Trefftz method, the field solution $u(x)$ is superimposed by the complete functions, $u_j(x)$, as follows:

$$u(x) = \sum_{j=1}^{2N_T+1} \omega_j u_j(x) \tag{7}$$

where $2N_T+1$ is the number of complete functions, ω_j is the jth unknown coefficient, $u_j(x)$ is the jth complementary set which satisfies the Laplace equation. For the interior problem, we choose 1, $\rho^n \sin(n\phi)$ and $\rho^n \cos(n\phi)$ ($n \in N$ and $0 < \rho < a$) to be the bases of the complementary set; and for the exterior problem we choose $\ln(\rho)$, $\rho^{-n} \sin(n\phi)$ and $\rho^{-n} \cos(n\phi)$ ($n \in N$ and $a < \rho < \infty$) to be the complete functions in the two-dimensional problem. Eq. (7) can be expressed by

$$u^I(\rho, \phi) = a_0 + \sum_{n=1}^{N_T} a_n \rho^n \cos(n\phi) + \sum_{n=1}^{N_T} b_n \rho^n \sin(n\phi), \quad 0 < \rho < a, \tag{8}$$

$$u^E(\rho, \phi) = a_0 \ln(\rho) + \sum_{n=1}^{N_T} a_n \rho^{-n} \cos(n\phi) + \sum_{n=1}^{N_T} b_n \rho^{-n} \sin(n\phi), \quad a < \rho < \infty. \tag{9}$$

By matching the boundary condition at $\rho = a$ and comparing the Eq. (8) with Eq. (6) for the interior problem, we obtain

$$a_0 = \bar{a}_0, \tag{10}$$

$$a_n = \frac{1}{a^n} \bar{a}_n, \quad n = 1, 2, \ldots, N_T, \tag{11}$$

$$b_n = \frac{1}{a^n} \bar{b}_n, \quad n = 1, 2, \ldots, N_T. \tag{12}$$

For the exterior problem by using Eq. (9), we have

$$a_0 = \frac{1}{\ln(a)} \bar{a}_0, \tag{13}$$

$$a_n = a^n \bar{a}_n, \quad n = 1, 2, \ldots, N_T, \tag{14}$$

$$b_n = a^n \bar{b}_n, \quad n = 1, 2, \ldots, N_T. \tag{15}$$

For the exterior problem with the radius of $a = 1$, it is interesting to find that the nonunique solution occurs since a_0 cannot be determined in Eq. (13) by using the Trefftz method.

3.2. Method of fundamental solutions (MFS)

In the MFS, the field solution $u(x)$ can be superimposed by $U(x, s_j)$ as follows:

$$u(x) = \sum_{j=1}^{N_M} c_j U(x, s_j), \quad s_j \in \Omega^e, \quad x \in \Omega \tag{16}$$

where N_M is the number of source points in the MFS, c_j is the jth unknown coefficient, s and x are the source point and collocation point, respectively, and Ω^e is the complementary domain. For the Laplace problem, we have the fundamental solution

$$U(x, s_j) = \ln(r), \tag{17}$$

where r is the distance between the source point and field point, we denote it as $r = |x - s_j|$. According to Eq. (17), Eq. (16) can be rewritten as

$$u(x) = \sum_{j=1}^{N_M} c_j U(s_j, x), \quad s_j \in \Omega^e. \tag{18}$$

The fundamental solution can be expressed by using the degenerate kernel

$$U(s, x) = U(R, \theta; \rho, \phi) = \ln(r)$$

$$= \begin{cases} U^I(s, x) = \ln(R) - \sum_{n=1}^{\infty} \frac{1}{n} \left(\frac{\rho}{R} \right)^n \cos(n(\theta - \phi)), & R > \rho, \\ U^E(s, x) = \ln(\rho) - \sum_{n=1}^{\infty} \frac{1}{n} \left(\frac{R}{\rho} \right)^n \cos(n(\theta - \phi)), & \rho > R, \end{cases} \tag{19}$$

where $s = (R, \theta)$ and $x = (\rho, \phi)$ are the polar coordinates of s and x, respectively. By substituting the degenerate form of the kernel function in Eq. (19) into Eq. (16), we have

$$u^I(\rho, \phi) = \sum_{j=1}^{N_M} c_j \left[\ln(R) - \sum_{n=1}^{\infty} \frac{1}{n} \left(\frac{\rho}{R} \right)^n \cos(n(\theta_j - \phi)) \right], \quad 0 < \rho < a, 0 < \phi < 2\pi \tag{20}$$

$$u^E(\rho, \phi) = \sum_{j=1}^{N_M} c_j \left[\ln(\rho) - \sum_{n=1}^{\infty} \frac{1}{n} \left(\frac{R}{\rho} \right)^n \cos(n(\theta_j - \phi)) \right], \quad a < \rho < \infty, 0 < \phi < 2\pi \tag{21}$$

where $\theta_j = \frac{2\pi}{N_M} j$. Eqs. (20) and (21) in the MFS imply the complete set of Eqs. (8) and (9) in the Trefftz method for the interior and exterior problems. By employing the property of trigonometric function and comparing the Eq. (6) with Eqs. (20) and (21) by truncating the higher order terms than N_M and matching the boundary condition, we have:

$$\bar{a}_0 = \sum_{j=1}^{N_M} c_j \ln(R), \tag{22}$$

$$\frac{\bar{a}_n}{a^n} = - \sum_{j=1}^{N_M} c_j \frac{1}{n} \left(\frac{1}{R} \right)^n \cos(n\theta_j), \quad n = 1, 2, \ldots, N_M, \tag{23}$$

$$\frac{\bar{b}_n}{a^n} = - \sum_{j=1}^{N_M} c_j \frac{1}{n} \left(\frac{1}{R} \right)^n \sin(n\theta_j), \quad n = 1, 2, \ldots, N_M. \tag{24}$$

For the exterior problem, we have

$$\bar{a}_0 = \sum_{j=1}^{N_M} c_j \frac{\ln(a)}{\ln(a)}, \tag{25}$$

$$a^n \bar{a}_n = \sum_{j=1}^{N_M} c_j \frac{1}{n} R^n \cos(n\theta_j), \quad n = 1, 2, \ldots, N_M, \tag{26}$$

$$a^n \bar{b}_n = \sum_{j=1}^{N_M} c_j \frac{1}{n} R^n \sin(n\theta_j), \quad n = 1, 2, \ldots, N_M. \tag{27}$$

Here, for the exterior problem with the radius of $a = 1$, it is interesting to find that the nonunique solution occurs not only in interior problem ($R = 1$) but also in the interior problem ($a = 1$), since c_j cannot be determined in Eq. (13) by using the MFS.

3.3. Connection between the Trefftz method and MFS

We can compare the coefficients in the Trefftz method and in the MFS for interior and exterior problems. By setting $2N_T + 1 = N_M = 2N + 1$ under the request of the same number of unknowns, the relationship between the unknown coefficients in the Trefftz method and the MFS can be written as:
Interior problem:

$$a_0 = \sum_{j=1}^{2N+1} c_j \ln(R), \tag{28}$$

$$a_n = -\sum_{j=1}^{2N+1} c_j \frac{1}{n} \left(\frac{1}{R}\right)^n \cos(n\theta_j), \quad n = 1, 2, \ldots, 2N + 1, \tag{29}$$

$$b_n = -\sum_{j=1}^{2N+1} c_j \frac{1}{n} \left(\frac{1}{R}\right)^n \sin(n\theta_j), \quad n = 1, 2, \ldots, 2N + 1, \tag{30}$$

Exterior problem:

$$a_0 = \sum_{j=1}^{2N+1} c_j \frac{\ln(a)}{\ln(a)}, \tag{31}$$

$$a_n = -\sum_{j=1}^{2N+1} c_j \frac{1}{n} R^n \cos(n\theta_j), \quad n = 1, 2, \ldots, 2N + 1, \tag{32}$$

$$b_n = -\sum_{j=1}^{2N+1} c_j \frac{1}{n} R^n \sin(n\theta_j), \quad n = 1, 2, \ldots, 2N + 1. \tag{33}$$

After comparing with the two solutions for the Trefftz method and the MFS, we can correlate as

$$\{\widetilde{u}\} = [K]\{\widetilde{v}\} \tag{34}$$

where

$$\widetilde{u} = \{a_0 \quad a_1 \quad b_1 \quad a_2 \quad b_2 \quad \cdots \quad a_N \quad b_N\}^{\mathrm{T}} \tag{35}$$

$$\widetilde{v} = \{c_1 \quad c_2 \quad c_3 \quad c_4 \quad c_5 \quad \cdots \quad c_{2N} \quad c_{2N+1}\}^{\mathrm{T}} \tag{36}$$

and the matrix $[K]$ for the interior case is

$$[K^I] = \begin{bmatrix} \ln(R) & \ln(R) & \ln(R) & \cdots & \ln(R) \\ \dfrac{-1}{R}\cos(\theta_1) & \dfrac{-1}{R}\cos(\theta_2) & \dfrac{-1}{R}\cos(\theta_3) & \cdots & \dfrac{-1}{R}\cos(\theta_{2N+1}) \\ \dfrac{-1}{R}\sin(\theta_1) & \dfrac{-1}{R}\sin(\theta_2) & \dfrac{-1}{R}\sin(\theta_3) & \cdots & \dfrac{-1}{R}\sin(\theta_{2N+1}) \\ \vdots & \vdots & \vdots & \ddots & \vdots \\ \dfrac{-1}{N}\left(\dfrac{1}{R}\right)^N\cos(N\theta_1) & \dfrac{-1}{N}\left(\dfrac{1}{R}\right)^N\cos(N\theta_2) & \dfrac{-1}{N}\left(\dfrac{1}{R}\right)^N\cos(N\theta_3) & \cdots & \dfrac{-1}{N}\left(\dfrac{1}{R}\right)^N\cos(N\theta_{2N+1}) \\ \dfrac{-1}{N}\left(\dfrac{1}{R}\right)^N\sin(N\theta_1) & \dfrac{-1}{N}\left(\dfrac{1}{R}\right)^N\sin(N\theta_2) & \dfrac{-1}{N}\left(\dfrac{1}{R}\right)^N\sin(N\theta_3) & \cdots & \dfrac{-1}{N}\left(\dfrac{1}{R}\right)^N\sin(N\theta_{2N+1}) \end{bmatrix} \tag{37}$$

and

$$[K^E] = \begin{bmatrix} 1 & 1 & 1 & \cdots & 1 \\ -R\cos(\theta_1) & -R\cos(\theta_2) & -R\cos(\theta_3) & \cdots & -R\cos(\theta_{2N+1}) \\ -R\sin(\theta_1) & -R\sin(\theta_2) & -R\sin(\theta_3) & \cdots & -R\sin(\theta_{2N+1}) \\ \vdots & \vdots & \vdots & \ddots & \vdots \\ \dfrac{-1}{N}R^N\cos(N\theta_1) & \dfrac{-1}{N}R^N\cos(N\theta_2) & \dfrac{-1}{N}R^N\cos(N\theta_3) & \cdots & \dfrac{-1}{N}R^N\cos(N\theta_{2N+1}) \\ \dfrac{-1}{N}R^N\sin(N\theta_1) & \dfrac{-1}{N}R^N\sin(N\theta_2) & \dfrac{-1}{N}R^N\sin(N\theta_3) & \cdots & \dfrac{-1}{N}R^N\sin(N\theta_{2N+1}) \end{bmatrix} \tag{38}$$

is for the exterior case. The relation of Eq. (34) is obtained to connect the Trefftz method and the MFS. We can decompose the matrix $[K]$ into two parts, one is the matrix, $[T_R]$, which depends on the radius of the source distribution; the other is the matrix, $[T_\theta]$, which depends on the angle of the source point (Fig. 1), as follows:

$$[K] = [T_R][T_\theta] \tag{39}$$

where

$$[T_R^I] = \begin{bmatrix} \ln(R) & 0 & 0 & 0 & \cdots & \cdots & 0 & 0 \\ 0 & \dfrac{-1}{R} & 0 & 0 & \cdots & \cdots & 0 & 0 \\ 0 & 0 & \dfrac{-1}{R} & 0 & \cdots & \cdots & \vdots & \vdots \\ \vdots & \vdots & \vdots & \dfrac{-1}{2}\left(\dfrac{1}{R}\right)^2 & \cdots & \cdots & \vdots & \vdots \\ \vdots & \vdots & \vdots & \vdots & \dfrac{-1}{2}\left(\dfrac{1}{R}\right)^2 & \cdots & \vdots & \vdots \\ \vdots & \vdots & \vdots & \vdots & \cdots & \ddots & 0 & 0 \\ 0 & 0 & 0 & \cdots & \cdots & \cdots & \dfrac{-1}{N}\left(\dfrac{1}{R}\right)^N & 0 \\ 0 & 0 & 0 & \cdots & \cdots & \cdots & 0 & \dfrac{-1}{N}\left(\dfrac{1}{R}\right)^N \end{bmatrix}_{(2N+1)\times(2N+1)} \tag{40}$$

is for the interior problem and

$$[T_R^E] = \begin{bmatrix} 1 & 0 & 0 & 0 & \cdots & \cdots & 0 & 0 \\ 0 & -R & 0 & 0 & \cdots & \cdots & 0 & 0 \\ 0 & 0 & -R & 0 & \cdots & \cdots & \vdots & \vdots \\ \vdots & \vdots & \vdots & \frac{-1}{2}R^2 & \cdots & \cdots & \vdots & \vdots \\ \vdots & \vdots & \vdots & \vdots & \frac{-1}{2}R^2 & \cdots & \vdots & \vdots \\ \vdots & \vdots & \vdots & \vdots & \cdots & \ddots & 0 & 0 \\ 0 & 0 & 0 & \cdots & \cdots & \cdots & \frac{-1}{N}R^N & 0 \\ 0 & 0 & 0 & \cdots & \cdots & \cdots & 0 & \frac{-1}{N}R^N \end{bmatrix}_{(2N+1)\times(2N+1)} \tag{41}$$

is for the exterior problem and

$$[T_\theta] = \begin{bmatrix} 1 & 1 & \cdots & \cdots & 1 \\ \cos(\theta_1) & \cos(\theta_2) & \cdots & \cdots & \cos(\theta_{2N+1}) \\ \sin(\theta_1) & \sin(\theta_2) & \cdots & \cdots & \sin(\theta_{2N+1}) \\ \cos(2\theta_1) & \cos(2\theta_2) & \cdots & \cdots & \cos(2\theta_{2N+1}) \\ \sin(2\theta_1) & \sin(2\theta_2) & \cdots & \cdots & \sin(2\theta_{2N+1}) \\ \vdots & \vdots & \ddots & \ddots & \vdots \\ \cos(N\theta_1) & \cos(N\theta_2) & \cdots & \cdots & \cos(N\theta_{2N+1}) \\ \sin(N\theta_1) & \sin(N\theta_2) & \cdots & \cdots & \sin(N\theta_{2N+1}) \end{bmatrix}_{(2N+1)\times(2N+1)}. \tag{42}$$

In Eq. (42), it is interesting to find

$$\det[T_\theta] = \frac{(2N+1)^{N+\frac{1}{2}}}{2^N} \tag{43}$$

due to the orthogonal property as follows:

$$[T_\theta][T_\theta]^{\mathrm{T}} = \begin{bmatrix} 2N+1 & 0 & \cdots & \cdots & 0 \\ 0 & \frac{2N+1}{2} & \cdots & \cdots & 0 \\ 0 & 0 & \frac{2N+1}{2} & \cdots & \vdots \\ \vdots & \vdots & \cdots & \ddots & 0 \\ 0 & 0 & \cdots & 0 & \frac{2N+1}{2} \end{bmatrix}_{(2N+1)\times(2N+1)}. \tag{44}$$

When the radius of the source location R moves far away from the real boundary or the number of the source points N_M becomes large, the condition number of $[K]$ matrix deteriorates. This is the reason why ill-posed behaviour is inherent in the MFS. In the $[T_R^I]$ matrix, it becomes singular at radius of one ($\ln(R) = 0$ for $R = 1$) which results in a degenerate scale in the MFS. For the exterior Dirichlet problem of radius one ($\ln(a) = 0$ for $a = 1$), the nonunique solution exists in Eq. (9) where a_0 cannot be determined. Even though the Trefftz method can not obtain the unique solution as shown in Eq. (13). This may explain why the transformation matrix between the MFS and the Trefftz method is nonsingular for the exterior problem. Degenerate scale in the MFS stems from the singular matrix. A detailed study of the degenerate scale in the MFS due to numerical nonuniqueness will be elaborated on later.

3.4. Discussion of the degenerate scale in the MFS for the Dirichlet problem

For the circular case with radius a, we can express $x = (\rho, \phi)$ and $s = (R, \theta)$ in terms of polar coordinate. Eqs. (20) and (21) can be expressed in terms of the degenerate kernel as below:

$$u^I(\rho, \phi) = \sum_{j=1}^{N_M} c_j \left[\ln(R) - \sum_{n=1}^{\infty} \frac{1}{n} \left(\frac{a}{R} \right)^n \cos(n(\theta_j - \phi)) \right], \quad 0 < \rho < a,\ 0 < \phi < 2\pi, \tag{45}$$

$$u^E(\rho, \phi) = \sum_{j=1}^{N_M} c_j \left[\ln(a) - \sum_{n=1}^{\infty} \frac{1}{n} \left(\frac{R}{a} \right)^n \cos(n(\theta_j - \phi)) \right], \quad a < \rho < \infty,\ 0 < \phi < 2\pi, \tag{46}$$

By matching the boundary condition, the MFS yields the following algebraic equation:

$$[U]\{\widetilde{c}\} = [T_\theta] \begin{Bmatrix} p_0 \\ p_1 \\ q_1 \\ \vdots \\ p_N \\ q_N \end{Bmatrix}. \tag{47}$$

Based on the circulants for the system of finite number degrees of freedom by locating uniformly $2N$ source points on a circular boundary, we have the influence matrix

$$[U] = \begin{bmatrix} a_0 & a_1 & a_2 & \cdots & a_{2N-1} \\ a_{2N-1} & a_0 & a_1 & \cdots & a_{2N-2} \\ a_{2N-2} & a_{2N-1} & a_0 & \cdots & a_{2N-3} \\ \vdots & \vdots & \vdots & \ddots & \vdots \\ a_1 & a_2 & a_3 & \cdots & a_0 \end{bmatrix}_{2N \times 2N} \tag{48}$$

where

$$a_m = U(R, \theta_m; \rho, 0), \quad m = 0, 1, 2, \ldots, 2N - 1 \tag{49}$$

in which $\theta_m = \frac{2\pi m}{2N}$, $\phi = 0$ without loss of generality. The matrix U in Eq. (48) is found to be circulant since the rotation symmetry for the influence coefficients is considered. By introducing the following bases for the circulants $1, (C_{2N})^1, (C_{2N})^2, \ldots, (C_{2N})^{2N-1}$, we can expand matrix U into

$$[U] = a_0 I + a_1 (C_{2N})^1 + a_2 (C_{2N})^2 + \cdots + a_{2N-1} (C_{2N})^{2N-1} \tag{50}$$

where I is an identity matrix and

$$(C_{2N})^1 = \begin{bmatrix} 0 & 1 & 0 & \cdots & 0 \\ 0 & 0 & 1 & \cdots & 0 \\ 0 & 0 & 0 & \cdots & 0 \\ \vdots & \vdots & \vdots & \ddots & \vdots \\ 1 & 0 & 0 & \cdots & 0 \end{bmatrix}_{2N \times 2N}. \tag{51}$$

Based on the circulant property, the spectral properties (eigenvalues) for the influence matrix, U, can be easily found as follows:

$$\lambda_k = a_0 + a_1 \alpha_k + a_2 \alpha_k^2 + \cdots + a_{2N-1} \alpha_k^{2N-1}, \quad k = 0, \pm 1, \pm 2, \ldots, \pm N - 1, N \tag{52}$$

where λ_k and α_k are the eigenvalues for the matrices U and $(C_{2N})^1$, respectively. It is easily found that the eigenvalues for the circulant C_{2N} is the root for $\alpha^{2N} = 1$ as shown below:

$$\alpha_k = e^{i \frac{2\pi k}{2N}}, \quad k = 0, \pm 1, \pm 2, \ldots, \pm N - 1, N. \tag{53}$$

Substituting Eq. (53) into Eq. (52), we have

$$\lambda_k = \sum_{m=0}^{2N-1} a_m \alpha_k^m = \sum_{m=0}^{2N-1} a_m e^{i\frac{2\pi mk}{2N}}. \tag{54}$$

According to the definition for in Eq. (49), we have

$$a_m = a_{2N-m}, \quad m = 0, 1, 2, \ldots, 2N - 1. \tag{55}$$

Substitution of Eqs. (53) and (55) yields

$$\lambda_k = \sum_{m=0}^{2N-1} a_m \cos(mk\Delta\theta). \tag{56}$$

Substituting a_m in the Eq. (49) into Eq. (56) and using the degenerate kernel of U in Eq. (19), the Riemann sum of infinite terms reduces to the following integral:

$$\lambda_k = \lim_{N\to\infty} \sum_{m=0}^{2N-1} U(m\Delta\theta, 0)\cos(mk\Delta\theta) \approx \frac{1}{\rho\Delta\theta} \int_0^{2\pi} U(\theta, 0)\cos(k\theta)\rho d\theta. \tag{57}$$

By using the degenerate kernel for $U(s, x)$ in Eq. (19) and the orthogonal conditions, Eq. (57) can be derived as

$$\lambda_k^I = \begin{cases} 2N\ln(R), & k = 0 \\ \dfrac{-2N}{|k|}\left(\dfrac{a}{R}\right)^{|k|}, & k = \pm 1, \pm 2, \ldots, \pm(N-1), N \end{cases} \tag{58}$$

for the interior problem, and

$$\lambda_k^E = \begin{cases} 2N\ln(a), & k = 0 \\ \dfrac{-2N}{|k|}\left(\dfrac{R}{a}\right)^{|k|}, & k = \pm 1, \pm 2, \ldots, \pm(N-1), N \end{cases} \tag{59}$$

for the exterior problem. Therefore, the determinant of matrix U can be represented by

$$\det[U^I] = (-2N)^{2N-1}\frac{2a\ln(R)}{R}\prod_{\beta=1}^{N-1}\left(\left(\frac{a}{R}\right)^{2\beta}\frac{1}{\beta^2}\right), \tag{60}$$

$$\det[U^E] = (-2N)^{2N-1}\frac{2R\ln(a)}{a}\prod_{\beta=1}^{N-1}\left(\left(\frac{R}{a}\right)^{2\beta}\frac{1}{\beta^2}\right). \tag{61}$$

According to Eqs. (60) and (61), we find that $\ln(R)$ and $\ln(a)$ are embedded in the determinant of influence matrices and the degenerate scale still occurs for the interior and exterior problems. Finally, it is obviously important to examine the occurring mechanism of the degenerate scale through Eqs. (60) and (61). After comparing the Eqs. (40) and (41) with the Eqs. (60) and (61) using the circulants, the same mechanism of the degenerate scale is obtained for the interior or exterior Laplace problem. Based on the successful experiences of the Laplace problem, we will consider the equivalence of the Trefftz method and MFS for the biharmonic problem in the next section. The degenerate scale will be examined for the biharmonic problem.

4. Connection between the Trefftz method and the MFS for biharmonic equations

4.1. Problem definition

Plate problem: Consider a clamped plate of radius a under uniformly distributed load $w(x)$ as shown in Fig. 3(a), the governing equation is

$$\nabla^4 u(x) = \frac{w(x)}{D}, \quad x \in \Omega, \tag{62}$$

where $u(x)$ is the lateral displacement of the circular plate, D is the flexural rigidity of the plate, Ω is the domain of interest. For simplicity, we set $w(x)$ is a constant of w. For the clamped case, the boundary conditions are

uniform pressure $w(x) = w$

$u = 0, \quad \theta = 0$

(a) Plate problem.

$u = \overline{u}, \quad \theta = \overline{\theta}$

(b) Stokes' flow problem.

a

$\Delta^2 u = 0$
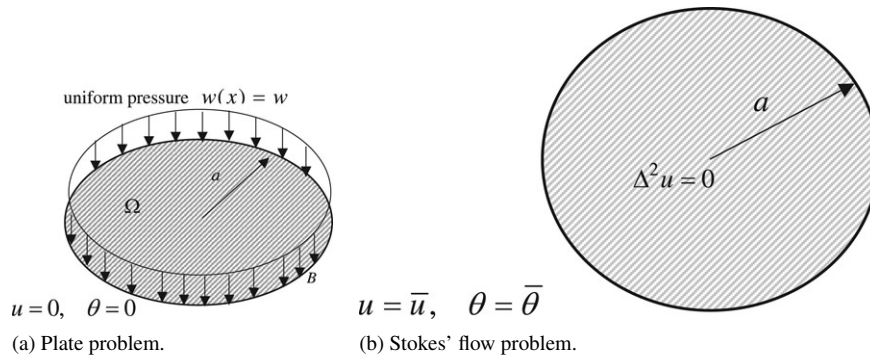
Fig. 3. Two kinds of physical problems for the biharmonic equation.

$$u(x) = 0, \qquad \theta(x) = 0, \quad x \in B, \tag{63}$$

where B is the boundary of the domain. Since Eq. (62) contains the body force term, the problem can be reformulated by using the splitting method

$$\nabla^4 u^*(x) = 0, \quad x \in \Omega, \tag{64}$$

and the boundary condition is changed to

$$u^*(x) = \frac{-wa^4}{64D}, \qquad \theta^*(x) = \frac{-wa^3}{16D}, \quad x \in B. \tag{65}$$

Stokes' flow problem: Consider the Stokes' flow problem with radius a as shown in Fig. 3(b), we have the governing equation as the same with Eq. (64) and the boundary conditions are

$$u^*(x) = \overline{u}, \qquad \frac{\partial u^*}{\partial n} = \overline{\theta}, \tag{66}$$

where $\overline{u}$ and $\overline{\theta}$ are specified. From the two different physical problems, we have the same governing equation and similar boundary conditions. The two physical problems have the same governing equation in Eq. (64) subject to essential boundary conditions of Eqs. (65) and (66), respectively. For the general form of boundary conditions,

$$u^*(a, \phi) = p_0 + \sum_{m=1}^{\infty} p_m \cos(m\phi) + \sum_{m=1}^{\infty} q_m \sin(m\phi), \tag{67}$$

$$\frac{\partial u^*(a, \phi)}{\partial n} = r_0 + \sum_{m=1}^{\infty} r_m \cos(m\phi) + \sum_{m=1}^{\infty} s_m \sin(m\phi) \tag{68}$$

we have an analytical solution for the biharmonic equation

$$u^*(\rho, \phi) = a_0 + \sum_{m=1}^{N_T} a_m \rho^m \cos(m\phi) + \sum_{m=1}^{N_T} b_m \rho^m \sin(m\phi) + c_0 \rho^2 + \sum_{m=1}^{N_T} c_m \rho^{m+2} \cos(m\phi)$$

$$+ \sum_{m=1}^{N_T} d_m \rho^{m+2} \sin(m\phi) \tag{69}$$

where

$$a_0 = p_0 - \frac{a}{2} r_0, \tag{70}$$

$$a_m = \frac{m+2}{2} a^{-m} p_m - \frac{1}{2} a^{1-m} r_m, \quad m = 1, 2, 3, \ldots, \tag{71}$$

$$b_m = \frac{m+2}{2} a^{-m} q_m - \frac{1}{2} a^{1-m} s_m, \quad m = 1, 2, 3, \ldots, \tag{72}$$

$$c_0 = \frac{1}{2a} r_0, \tag{73}$$

$$c_m = \frac{-m}{2} a^{-m-2} p_m - \frac{1}{2} a^{-1-m} r_m, \quad m = 1, 2, 3, \ldots, \tag{74}$$

$$d_m = \frac{-m}{2} a^{-m-2} q_m - \frac{1}{2} a^{-1-m} s_m, \quad m = 1, 2, 3, \ldots, \tag{75}$$

4.2. Trefftz method

By using the Trefftz method for the biharmonic equation, we choose 1, ρ^2, $\rho^m \cos(m\phi)$, $\rho^m \sin(m\phi)$, $\rho^{m+2} \cos(m\phi)$, $\rho^{m+2} \sin(m\phi)$ to be the bases of the complementary set. Eq. (1) can be expressed by

$$u^*(\rho, \phi) = a_0 + \sum_{m=1}^{N_T} a_m \rho^m \cos(m\phi) + \sum_{m=1}^{N_T} b_m \rho^m \sin(m\phi)$$
$$+ c_0 \rho^2 + \sum_{m=1}^{N_T} c_m \rho^{m+2} \cos(m\phi) + \sum_{m=1}^{N_T} d_m \rho^{m+2} \sin(m\phi), \tag{76}$$

$$\theta^*(\rho, \phi) = \sum_{m=1}^{N_T} a_m m \rho^{m-1} \cos(m\phi) + \sum_{m=1}^{N_T} b_m m \rho^{m-1} \sin(m\phi) + c_0(2\rho)$$
$$+ \sum_{m=1}^{N_T} c_m (m+2) \rho^{m+1} \cos(m\phi) + \sum_{m=1}^{N_T} d_m (m+2) \rho^{m+1} \sin(m\phi), \tag{77}$$

where a_0, a_m, b_m, c_0, c_m and d_m are the coefficients of the Trefftz method. By matching the boundary conditions of Eqs. (67) and (68) at $\rho = a$, we have

$$\begin{Bmatrix} a_0 \\ a_1 \\ b_1 \\ \vdots \\ a_m \\ b_m \\ c_0 \\ c_1 \\ d_1 \\ \vdots \\ c_m \\ d_m \end{Bmatrix} = \begin{bmatrix} 1 & 0 & 0 & \cdots & 0 & 0 & \frac{-a}{2} & 0 & 0 & \cdots & 0 & 0 \\ 0 & \frac{3}{2}a^{-1} & 0 & \cdots & 0 & 0 & 0 & \frac{-1}{2} & 0 & \cdots & 0 & 0 \\ 0 & 0 & \frac{3}{2}a^{-1} & \cdots & 0 & 0 & 0 & 0 & \frac{-1}{2} & \cdots & 0 & 0 \\ \vdots & \vdots & \vdots & \ddots & \vdots & \vdots & \vdots & \vdots & \vdots & \ddots & \vdots & \vdots \\ 0 & 0 & 0 & \cdots & \frac{m+2}{2}a^{-m} & 0 & 0 & 0 & 0 & \cdots & \frac{-1}{2}a^{1-m} & 0 \\ 0 & 0 & 0 & \cdots & 0 & \frac{m+2}{2}a^{-m} & 0 & 0 & 0 & \cdots & 0 & \frac{-1}{2}a^{1-m} \\ 0 & 0 & 0 & \cdots & 0 & 0 & \frac{1}{2a} & 0 & 0 & \cdots & 0 & 0 \\ 0 & \frac{-1}{2}a^{-3} & 0 & \cdots & 0 & 0 & 0 & \frac{1}{2}a^2 & 0 & \cdots & 0 & 0 \\ 0 & 0 & \frac{-1}{2}a^{-3} & \cdots & 0 & 0 & 0 & 0 & \frac{1}{2}a^2 & \cdots & 0 & 0 \\ \vdots & \vdots & \vdots & \ddots & \vdots & \vdots & \vdots & \vdots & \vdots & \ddots & \vdots & \vdots \\ 0 & 0 & 0 & \cdots & \frac{-m}{2}a^{-m-2} & 0 & 0 & 0 & 0 & \cdots & \frac{1}{2}a^{-m-1} & 0 \\ 0 & 0 & 0 & \cdots & 0 & \frac{-m}{2}a^{-m-2} & 0 & 0 & 0 & \cdots & 0 & \frac{1}{2}a^{-m-1} \end{bmatrix} \begin{Bmatrix} p_0 \\ p_1 \\ q_1 \\ \vdots \\ p_m \\ q_m \\ r_0 \\ r_1 \\ s_1 \\ \vdots \\ r_m \\ s_m \end{Bmatrix}. \tag{78}$$

Eq. (78) is found to be the same as Eqs. (70)–(75). Therefore, we can construct the analytical solution through the Trefftz method.

4.3. Method of fundamental solutions

We use the MFS to solve the same problem. According to the Eq. (2), the slope field can be obtained as

$$
\begin{aligned}
\theta(x) &= \frac{\partial u(x)}{\partial n_x} = \sum_{j=1}^{N_M} v_j \frac{\partial U(x, s_j)}{\partial n_x} \\
&= \sum_{j=1}^{N_M} v_j L(s, x), \quad s_j \in D^e.
\end{aligned}
\tag{79}
$$

The fundamental solution can be expressed by using the degenerate kernel as follows:

$$
\begin{aligned}
U^I(\rho, \phi; R, \theta) &= r^2 \ln(r) \\
&= [\rho^2 + R^2 - 2\rho R \cos(\theta - \phi)] \left[\ln(R) - \sum_{m=1}^{\infty} \frac{1}{m} \left(\frac{\rho}{R} \right)^m \cos m(\theta - \phi) \right] \\
&= \rho^2(1 + \ln(R)) + R^2 \ln(R) - 2\rho R \ln(R) \cos\theta \cos\phi - 2\rho R \ln(R) \sin\theta \sin\phi \\
&\quad - \rho R \cos\theta \cos\phi - \rho R \sin\theta \sin\phi - \frac{\rho^3}{2R} \cos\theta \cos\phi - \frac{\rho^3}{2R} \sin\theta \sin\phi \\
&\quad - \sum_{m=2}^{\infty} \frac{\rho^m}{R^{m-2}} \left[\frac{\rho^2}{m(m+1)R^2} - \frac{1}{m(m-1)} \right] \cos m\theta \cos m\phi \\
&\quad - \sum_{m=2}^{\infty} \frac{\rho^m}{R^{m-2}} \left[\frac{\rho^2}{m(m+1)R^2} - \frac{1}{m(m-1)} \right] \sin m\theta \sin m\phi, \quad R > \rho
\end{aligned}
\tag{80}
$$

and

$$
\begin{aligned}
L^I(\rho, \phi; R, \theta) &= \frac{\partial U^I(\rho, \phi; R, \theta)}{\partial n_x} \\
&= 2\rho(1 + \ln(R)) - 2R \ln R \cos\theta \cos\phi - 2R \ln R \sin\theta \sin\phi - R \cos\theta \cos\phi \\
&\quad - R \sin\theta \sin\phi - \frac{3\rho^2}{2R} \cos\theta \cos\phi - \frac{3\rho^2}{2R} \sin\theta \sin\phi \\
&\quad - \sum_{m=2}^{\infty} \frac{\rho^{m+1}}{R^m} \frac{m+2}{m(m+1)} \cos m\theta \cos m\phi - \sum_{m=2}^{\infty} \frac{\rho^{m+1}}{R^m} \frac{m+2}{m(m+1)} \sin m\theta \sin m\phi \\
&\quad + \sum_{m=2}^{\infty} \frac{\rho^{m-1}}{R^{m-2}} \frac{1}{m-1} \cos m\theta \cos m\phi + \sum_{m=2}^{\infty} \frac{\rho^{m-1}}{R^{m-2}} \frac{1}{m-1} \sin m\theta \sin m\phi, \quad R > \rho.
\end{aligned}
\tag{81}
$$

By substituting Eqs. (80) and (81) into Eqs. (2) and (79), respectively, and matching the boundary conditions of Eqs. (67) and (68), we have

$$
\sum_{j=1}^{N_M} v_j (R^2 \ln R) = p_0 - \frac{a}{2} r_0,
\tag{82}
$$

$$
-\sum_{j=1}^{N_M} v_j [R(1 + 2\ln R)] \cos\theta_j = \frac{3}{2} a^{-1} p_1 - \frac{1}{2} r_1,
\tag{83}
$$

$$
-\sum_{j=1}^{N_M} v_j [R(1 + 2\ln R)] \sin\theta_j = \frac{3}{2} a^{-1} q_1 - \frac{1}{2} s_1,
\tag{84}
$$

$$
-\sum_{j=1}^{N_M} v_j \frac{1}{m(m-1)} \frac{1}{R^{m-2}} \cos m\theta_j = \frac{m+2}{2} a^{-m} p_m - \frac{1}{2} a^{1-m} r_m,
\tag{85}
$$

$$-\sum_{j=1}^{N_M} v_j \frac{1}{m(m-1)} \frac{1}{R^{m-2}} \sin m\theta_j = \frac{m+2}{2} a^{-m} q_m - \frac{1}{2} a^{1-m} s_m, \tag{86}$$

$$\sum_{j=1}^{N_M} v_j (1 + \ln R) = \frac{1}{2a} c_0, \tag{87}$$

$$\sum_{j=1}^{N_M} v_j \frac{-1}{2R} \cos \theta_j = \frac{-1}{2} a^{-3} p_1 + \frac{1}{2} a^{-2} r_1, \tag{88}$$

$$\sum_{j=1}^{N_M} v_j \frac{-1}{2R} \sin \theta_j = \frac{-1}{2} a^{-3} q_1 + \frac{1}{2} a^{-2} s_1, \tag{89}$$

$$\sum_{j=1}^{N_M} v_j \frac{-1}{R^m} \frac{1}{m(m+1)} \cos m\theta_j = \frac{-m}{2} a^{-m-2} p_m + \frac{1}{2} a^{-m-1} r_m, \tag{90}$$

$$\sum_{j=1}^{N_M} v_j \frac{-1}{R^m} \frac{1}{m(m+1)} \sin m\theta_j = \frac{-m}{2} a^{-m-2} q_m + \frac{1}{2} a^{-m-1} s_m. \tag{91}$$

Eqs. (82)–(91) can be rewritten as

$$[K]\{\tilde{v}\} = \begin{bmatrix} 1 & 0 & 0 & \cdots & 0 & 0 & \frac{-a}{2} & 0 & 0 & \cdots & 0 & 0 \\ 0 & \frac{3}{2}a^{-1} & 0 & \cdots & 0 & 0 & 0 & \frac{-1}{2} & 0 & \cdots & 0 & 0 \\ 0 & 0 & \frac{3}{2}a^{-1} & \cdots & 0 & 0 & 0 & 0 & \frac{-1}{2} & \cdots & 0 & 0 \\ \vdots & \vdots & \vdots & \ddots & \vdots & \vdots & \vdots & \vdots & \vdots & \ddots & \vdots & \vdots \\ 0 & 0 & 0 & \cdots & \frac{m+2}{2}a^{-m} & 0 & 0 & 0 & 0 & \cdots & \frac{-1}{2}a^{1-m} & 0 \\ 0 & 0 & 0 & \cdots & 0 & \frac{m+2}{2}a^{-m} & 0 & 0 & 0 & \cdots & 0 & \frac{-1}{2}a^{1-m} \\ 0 & 0 & 0 & \cdots & 0 & 0 & \frac{1}{2a} & 0 & 0 & \cdots & 0 & 0 \\ 0 & \frac{-1}{2}a^{-3} & 0 & \cdots & 0 & 0 & 0 & \frac{1}{2}a^2 & 0 & \cdots & 0 & 0 \\ 0 & 0 & \frac{-1}{2}a^{-3} & \cdots & 0 & 0 & 0 & 0 & \frac{1}{2}a^2 & \cdots & 0 & 0 \\ \vdots & \vdots & \vdots & \ddots & \vdots & \vdots & \vdots & \vdots & \vdots & \ddots & \vdots & \vdots \\ 0 & 0 & 0 & \cdots & \frac{-m}{2}a^{-m-2} & 0 & 0 & 0 & 0 & \cdots & \frac{1}{2}a^{-m-1} & 0 \\ 0 & 0 & 0 & \cdots & 0 & \frac{-m}{2}a^{-m-2} & 0 & 0 & 0 & \cdots & 0 & \frac{1}{2}a^{-m-1} \end{bmatrix} \begin{Bmatrix} p_0 \\ p_1 \\ q_1 \\ \vdots \\ p_m \\ q_m \\ r_0 \\ r_1 \\ s_1 \\ \vdots \\ r_m \\ s_m \end{Bmatrix} \tag{92}$$

where

$$[K] = \begin{bmatrix} \langle w_1 \rangle \\ \langle w_2 \rangle \\ \vdots \\ \vdots \\ \langle w_{N_M} \rangle \end{bmatrix}_{N_M \times N_M} \tag{93}$$

$$\tilde{v} = \begin{Bmatrix} v_1 & v_2 & v_3 & v_4 & v_5 & \cdots & v_{N_M-1} & v_{N_M} \end{Bmatrix}^{\mathrm{T}} \tag{94}$$

in which

$$\langle w_1 \rangle = R^2 \ln R[1, 1, \ldots, 1],$$
$$\langle w_2 \rangle = -R(1 + 2\ln R)[\cos(\theta_1), \cos(\theta_2), \ldots, \cos(\theta_{N_M})],$$
$$\langle w_3 \rangle = -R(1 + 2\ln R)[\sin(\theta_1), \sin(\theta_2), \ldots, \sin(\theta_{N_M})],$$
$$\vdots$$
$$\langle w_{\frac{N_M}{2}} \rangle = \frac{1}{N(N-1)} \left(\frac{1}{R}\right)^{N-2} [\cos(N\theta_1), \cos(N\theta_2), \ldots, \cos(N\theta_{N_M})],$$
$$\langle w_{\frac{N_M}{2}+1} \rangle = \frac{1}{N(N-1)} \left(\frac{1}{R}\right)^{N-2} [\sin(N\theta_1), \sin(N\theta_2), \ldots, \sin(N\theta_{N_M})],$$
$$\langle w_{\frac{N_M}{2}+2} \rangle = (1 + \ln(R))[1, 1, \ldots, 1], \tag{95}$$
$$\langle w_{\frac{N_M}{2}+3} \rangle = \frac{-1}{2R}[\cos(\theta_1), \cos(\theta_2), \ldots, \cos(\theta_{N_M})],$$
$$\langle w_{\frac{N_M}{2}+4} \rangle = \frac{-1}{2R}[\sin(\theta_1), \sin(\theta_2), \ldots, \sin(\theta_{N_M})],$$
$$\vdots$$
$$\langle w_{N_M-1} \rangle = \frac{1}{N(N+1)} \frac{-1}{R^N} [\cos(N\theta_1), \cos(N\theta_2), \ldots, \cos(N\theta_{N_M})],$$
$$\langle w_{N_M} \rangle = \frac{1}{N(N+1)} \frac{-1}{R^N} [\sin(N\theta_1), \sin(N\theta_2), \ldots, \sin(N\theta_{N_M})].$$

Therefore, we can compare the Eq. (78) in the Trefftz method with Eq. (92) in the MFS. By setting $4N_T + 2 = N_M = 4N + 2$ under the request of the same number of unknowns, the relationship between the coefficients in the Trefftz method and the MFS can be connected by

$$\begin{Bmatrix} p_0 \\ p_1 \\ q_1 \\ \vdots \\ p_N \\ q_N \\ r_0 \\ r_1 \\ s_1 \\ \vdots \\ r_N \\ s_N \end{Bmatrix}_{(4N+2)\times 1} = [K]_{(4N+2)\times(4N+2)} \begin{Bmatrix} v_1 \\ v_2 \\ v_3 \\ v_4 \\ \vdots \\ \vdots \\ \vdots \\ \vdots \\ \vdots \\ \vdots \\ v_{4N+1} \\ v_{4N+2} \end{Bmatrix}_{(4N+2)\times 1} \tag{96}$$

where the left-hand side is the column vector of the Trefftz coefficients and the right-hand side is the column vector of the MFS coefficients. The $[K]$ matrix in Eq. (96) can be decomposed to

$$[K] = [T_R][T_\theta] \tag{97}$$

where

$[T_R] =$

$$
\begin{bmatrix}
R^2 \ln R & 0 & 0 & 0 & 0 & 0 & 0 & 0 & 0 & 0 & 0 & 0 \\
0 & -R(1+2\ln R) & 0 & 0 & 0 & 0 & 0 & 0 & 0 & 0 & 0 & 0 \\
0 & 0 & -R(1+2\ln R) & 0 & 0 & 0 & 0 & 0 & 0 & 0 & 0 & 0 \\
0 & 0 & 0 & \ddots & 0 & 0 & 0 & 0 & 0 & 0 & 0 & 0 \\
0 & 0 & 0 & 0 & \frac{1}{R^{N-2}N(N-1)} & 0 & 0 & 0 & 0 & 0 & 0 & 0 \\
0 & 0 & 0 & 0 & 0 & \frac{1}{R^{N-2}N(N-1)} & 0 & 0 & 0 & 0 & 0 & 0 \\
0 & 0 & 0 & 0 & 0 & 0 & 1+\ln R & 0 & 0 & 0 & 0 & 0 \\
0 & 0 & 0 & 0 & 0 & 0 & 0 & \frac{-1}{2R} & 0 & 0 & 0 & 0 \\
0 & 0 & 0 & 0 & 0 & 0 & 0 & 0 & \frac{-1}{2R} & 0 & 0 & 0 \\
0 & 0 & 0 & 0 & 0 & 0 & 0 & 0 & 0 & \ddots & 0 & 0 \\
0 & 0 & 0 & 0 & 0 & 0 & 0 & 0 & 0 & 0 & \frac{1}{R^{N}N(N+1)} & 0 \\
0 & 0 & 0 & 0 & 0 & 0 & 0 & 0 & 0 & 0 & 0 & \frac{1}{R^{N}N(N+1)}
\end{bmatrix}
$$

(98)

and

$$
[T_\theta] =
\begin{bmatrix}
1 & 1 & \cdots & \cdots & 1 & 1 \\
\cos\theta_1 & \cos\theta_2 & \cdots & \cdots & \cos\theta_{4N+1} & \cos\theta_{4N+2} \\
\sin\theta_1 & \sin\theta_2 & \cdots & \cdots & \sin\theta_{4N+1} & \sin\theta_{4N+2} \\
\vdots & \vdots & \ddots & \ddots & \vdots & \vdots \\
\cos N\theta_1 & \cos N\theta_2 & \cdots & \cdots & \cos N\theta_{4N+1} & \cos N\theta_{4N+2} \\
\sin N\theta_1 & \sin N\theta_2 & \cdots & \cdots & \sin N\theta_{4N+1} & \sin N\theta_{4N+2} \\
1 & 1 & \cdots & \cdots & 1 & 1 \\
\cos\theta_1 & \cos\theta_2 & \cdots & \cdots & \cos\theta_{4N+1} & \cos\theta_{4N+2} \\
\sin\theta_1 & \sin\theta_2 & \cdots & \cdots & \sin\theta_{4N+1} & \sin\theta_{4N+2} \\
\vdots & \vdots & \ddots & \ddots & \vdots & \vdots \\
\cos N\theta_1 & \cos N\theta_2 & \cdots & \cdots & \cos N\theta_{4N+1} & \cos N\theta_{4N+2} \\
\sin N\theta_1 & \sin N\theta_2 & \cdots & \cdots & \sin N\theta_{4N+1} & \sin N\theta_{4N+2}
\end{bmatrix}.
$$

(99)

It is interesting to find that T_R is a diagonal matrix of dimension $(4N+2)$ by $(4N+2)$ and T_θ is an orthogonal matrix. The determinant of $[T_\theta]$ can be obtained

$$\det[T_\theta] = 2(2N+1)^{2N+1} \tag{100}$$

due to the orthogonal property as shown below:

$$
[T_\theta]^{\mathrm{T}}[T_\theta] =
\begin{bmatrix}
4N+2 & 0 & 0 & 0 & 0 & 0 & 0 & 0 \\
0 & 2N+1 & 0 & 0 & 0 & 0 & 0 & 0 \\
0 & 0 & \ddots & 0 & 0 & 0 & 0 & 0 \\
0 & 0 & 0 & 2N+1 & 0 & 0 & 0 & 0 \\
0 & 0 & 0 & 0 & 4N+2 & 0 & 0 & 0 \\
0 & 0 & 0 & 0 & 0 & 2N+1 & 0 & 0 \\
0 & 0 & 0 & 0 & 0 & 0 & \ddots & 0 \\
0 & 0 & 0 & 0 & 0 & 0 & 0 & 2N+1
\end{bmatrix}_{(4N+2)\times(4N+2)}.
$$

(101)

If the $[K]$ matrix is nonsingular, the equivalence between the two methods is proved. The singular $[K]$ matrix results in the problem of solvability using the MFS since $[K]$ cannot be invertible. This is numerically realizable instead of physical phenomena. The degenerate scale occurs at the three locations $R = \mathrm{e}^0, \mathrm{e}^{\frac{-1}{2}}, \mathrm{e}^{-1}$ since $\ln R$, $1 + \ln R$ and $1 + 2\ln R$ in Eq. (98) are zeros. A detailed study for the degenerate scale due to the phenomenon of the numerical nonuniqueness was noted in [4].

(a) Interior problem.

(b) Exterior problem.

Exact solution: $\dfrac{2}{\pi}\tan^{-1}(\dfrac{-2y}{1-x^2-y^2})$

Exact solution: $\dfrac{2}{\pi}\tan^{-1}(\dfrac{2y}{x^2+y^2-1})$
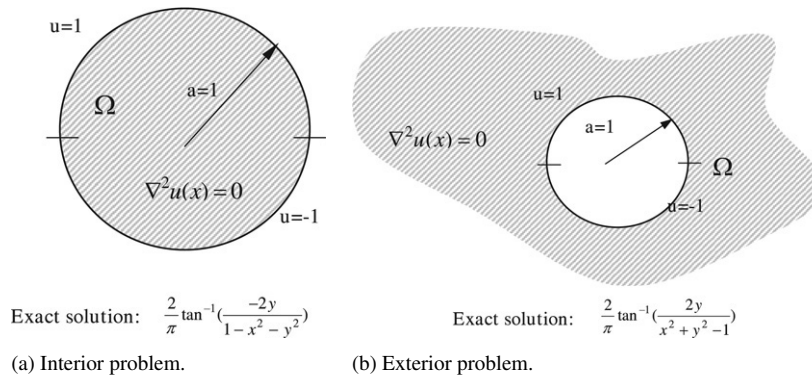
Fig. 4. Problem statement for the Laplace problem with the boundary condition ($u(x) = 1$ for upper-half circular boundary and $u(x) = -1$ for lower half circular boundary).

5. Numerical examples and discussion

Several problems subject to different boundary conditions for the interior and exterior problems are considered. Also, the doubly-connected problems with an annular domain and an eccentric case are solved by using the Trefftz method and the MFS.

5.1. Simply-connected problems

Consider the circular Laplace problem, we have the boundary condition with $u(x) = 1$ for the upper half circular boundary and $u(x) = -1$ for the lower half circular boundary for the interior and exterior problems. For simplicity, we set the radius $a = 1$ as shown in Fig. 4(a) and (b). By using the Trefftz method and MFS, we have the results in Figs. 5 and 6 for the interior and exterior problems. Besides, the solution of the boundary element method is also obtained. The number of complete functions in the Trefftz method are $N_T = 8, 16, 30$ and 50 terms. The number of source points in the MFS are $N_M = 17, 33, 61$ and 101 terms. Good agreement is made by comparing the Trefftz method, MFS and BEM with analytical solution separately.

Under the same unknowns ($N_M = 2N_T + 1 = 2N + 1$) in Figs. 5 and 6, we observe that the accuracy and efficiency of the MFS are better than the Trefftz method straightforwardly.

5.2. Multiply-connected problems

Annular case: We consider the Laplace annular problem with the radius a_1 and a_2 ($a_1 = 1, a_2 = 2.5$) as shown in Fig. 7. By selecting the source location of $R_1 = 0.9$ and $R_2 = 2.6$ in the MFS, the results are shown in Fig. 8. Good agreement is made after comparing with the exact solution in Fig. 9 (b). Also the Trefftz method obtained the similar results shown in Fig. 9.
Eccentric case: For the eccentric case in Fig. 10, the same technique is used. By choosing the different source locations in the MFS, the results are shown in Fig. 11(a), (b) and (c). Good agreement is made after comparing with the exact solution in Fig. 11(d). In addition, the Trefftz method can obtain the good results as shown in Fig. 12.

5.3. Discussion of the error analysis and optimal source positions

From the mathematical point of view, we verified the equivalence of two methods. Although, the Trefftz method and MFS are proved to be mathematically equivalent, their numerical behaviour is different to the varied condition number of the influence matrix of MFS and mapping matrix as shown in Fig. 13. They are different in the numerical implementation since unknown coefficients are not the same. Based on the simply-connected case in Fig. 4(a), the best location of source point can be chosen by detecting the condition number of mapping matrix shown in Fig. 13. The condition number for the influence matrix of MFS is also detected. The larger condition number will result in numerical instability. In the test example, the condition number doesn't deteriorate very much when source points are distributed in the range of $1 < R < 3$. The significant number of digital computer can cover the ill-posedness of
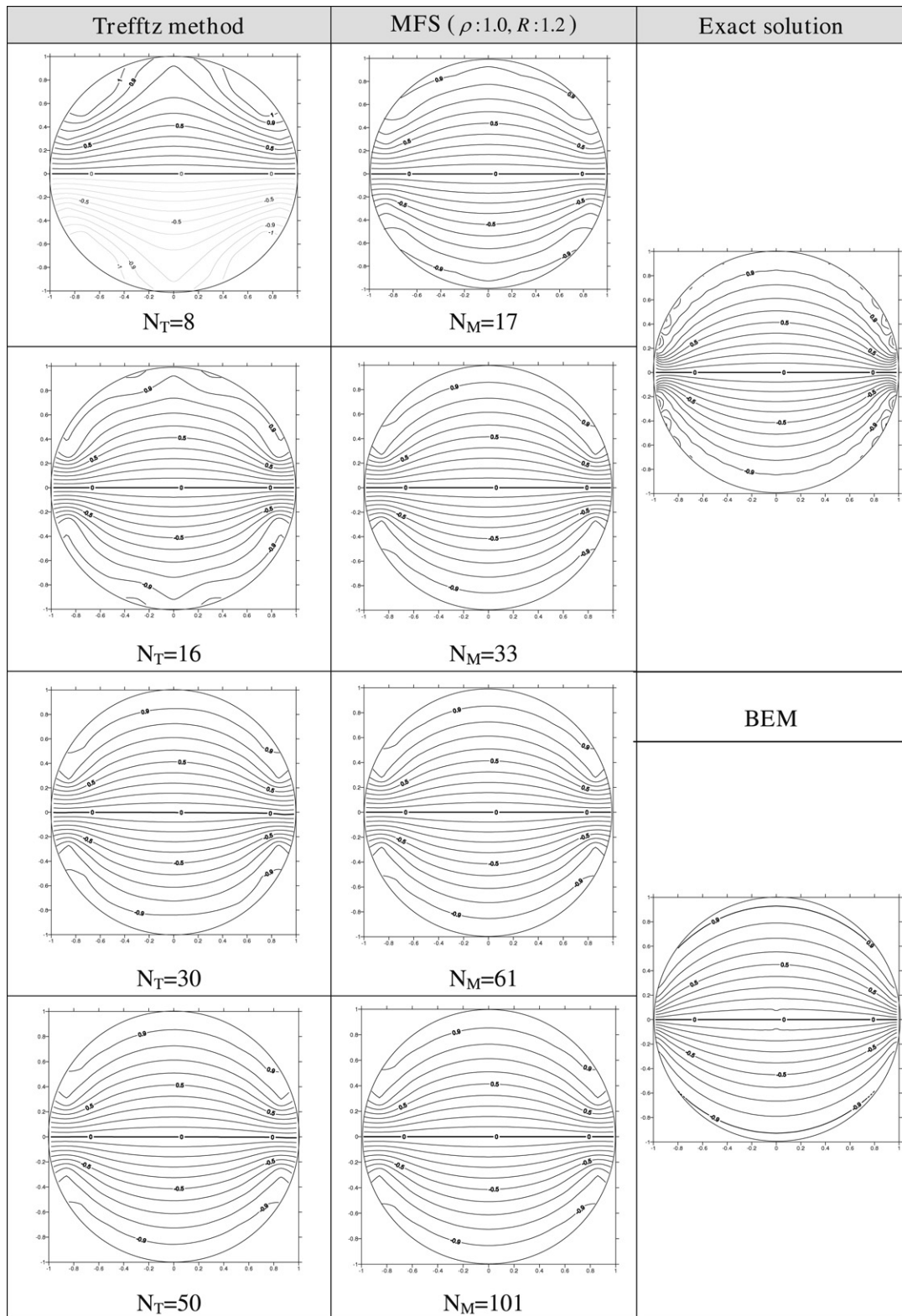
Fig. 5. Contour plots for the interior Laplace problem using the Trefftz method and MFS.

Trefftz method (add rigid body term 1.0)	MFS (ρ : 1.0, R : 0.8)	Exact solution
$N_T=8$	$N_M=17$	
$N_T=16$	$N_M=33$	
$N_T=30$	$N_M=61$	**BEM**
$N_T=50$	$N_M=101$	
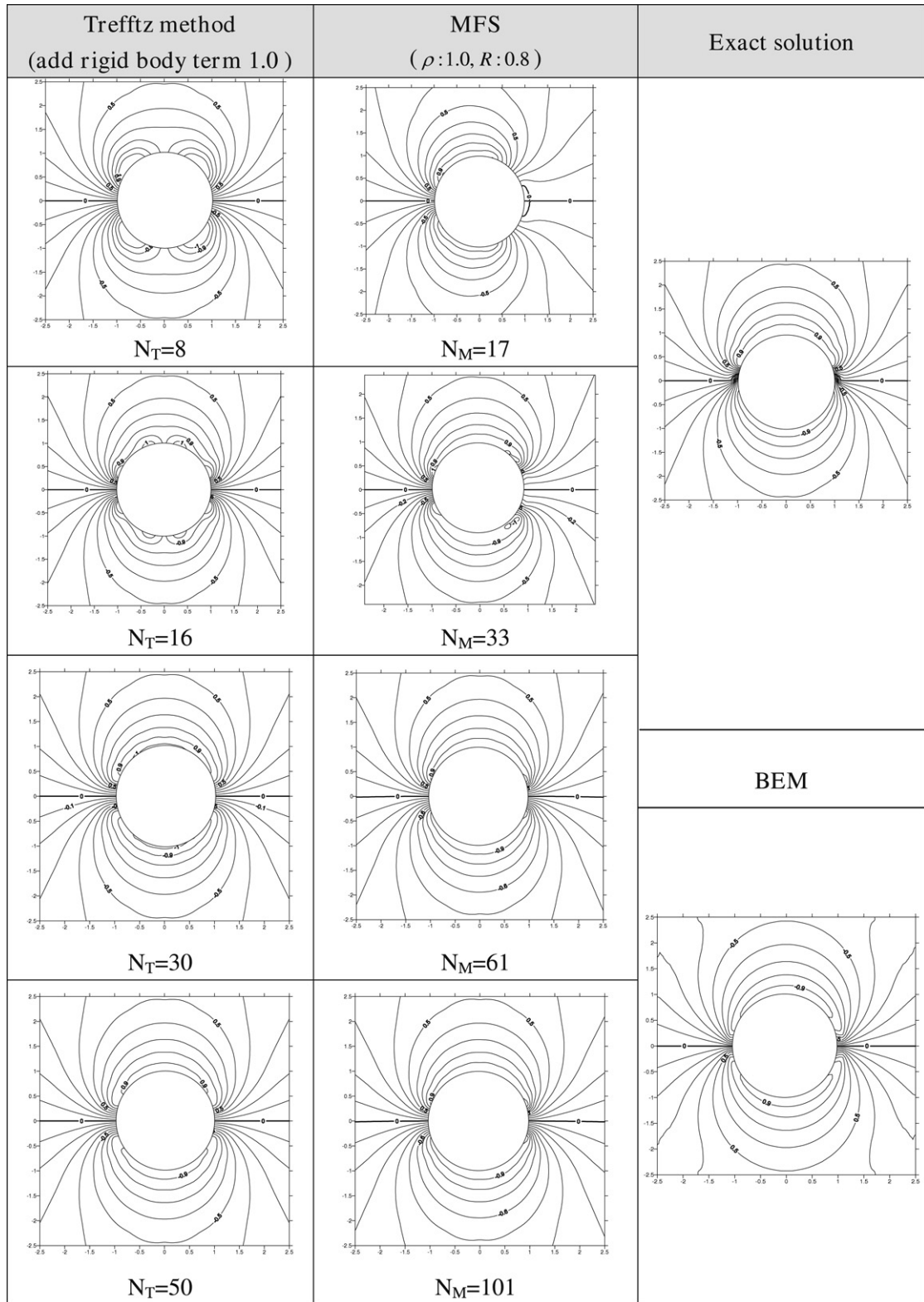
Fig. 6. Contour plots for the exterior Laplace problem using the Trefftz method and MFS.
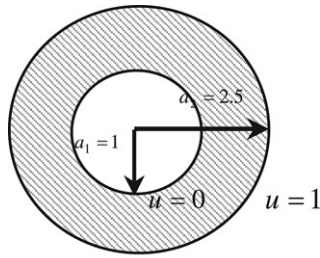
Exact solution: $u(\rho,\phi) = \dfrac{\ln \rho}{\ln 2.5}$

Fig. 7. Laplace equation of an annular domain.
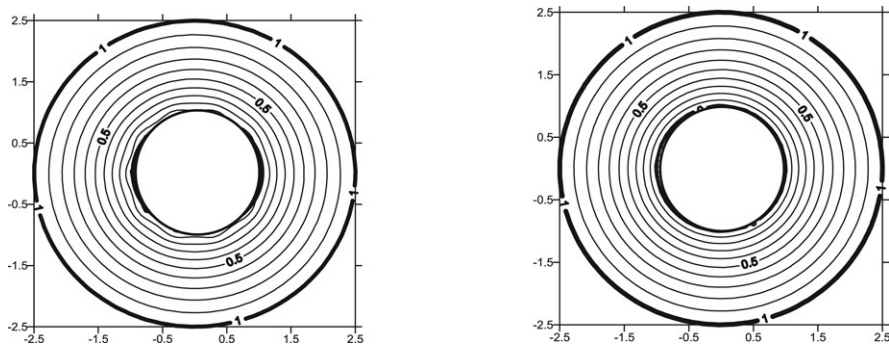
Fig. 8. Contour plots for the annular circle using the MFS (inner: $R_1 = 0.9$, 20 points; outer: $R_2 = 2.6$, 60 points).

(a) Numerical solution.   (b) Exact solution.
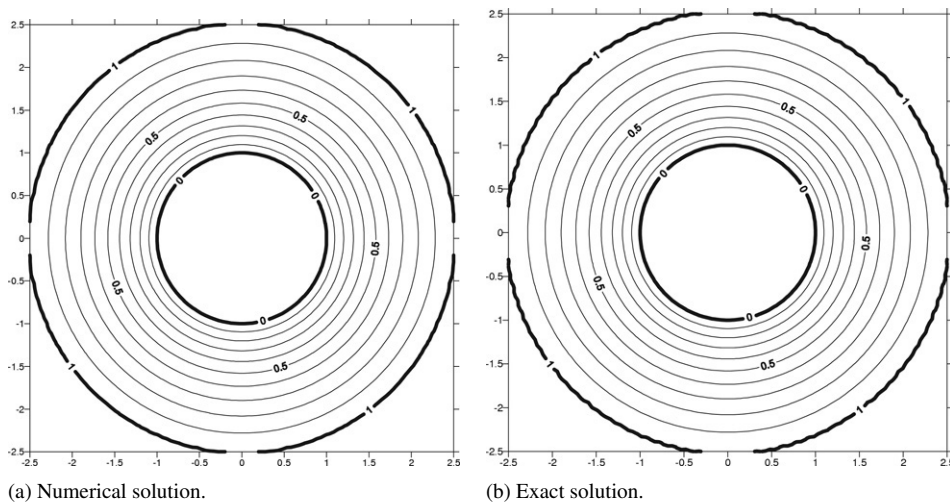
Fig. 9. Contour plots for the annular circle using the Trefftz method (26 points).

large condition number. Since the MFS is one kind of radial basis function, the influence matrix is constructed from a distance of two points. For the problem of complex geometry, MFS is more flexible to distribute the source points with respect to the given complex boundary for capturing the solution. However, the Trefftz method may be suitable for certain problems (rectangle or circle) with a continuous boundary condition using the corresponding T-complete functions (Cartesian or polar system). Different radii were also tested and the best result for the MFS is chosen when the source points are distributed at a radius of 1.2 as shown in Fig. 14. It indicates that the optimal location of

Exact solution $u(\rho, \phi) = \dfrac{1}{2\ln 2} \ln\{\dfrac{16\rho^2 + 1 + 8\rho\cos\phi}{\rho^2 + 16 + 8\rho\cos\phi}\}$
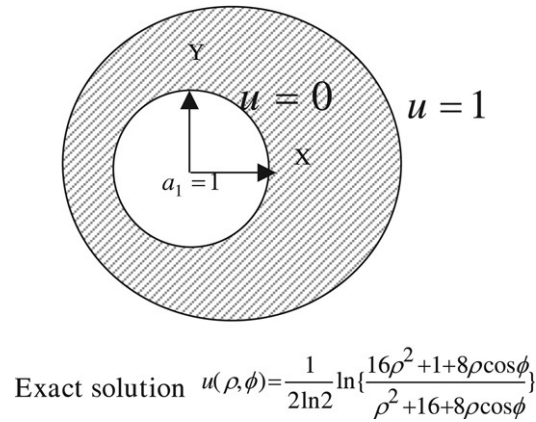
Fig. 10. Laplace equation of the eccentric case.

(a) $R_1 = 0.9, R_2 = 2.6$.

(b) $R_1 = 0.9, R_2 = 3.0$.

(c) $R_1 = 0.9, R_2 = 4.0$.

(d) Exact solution.
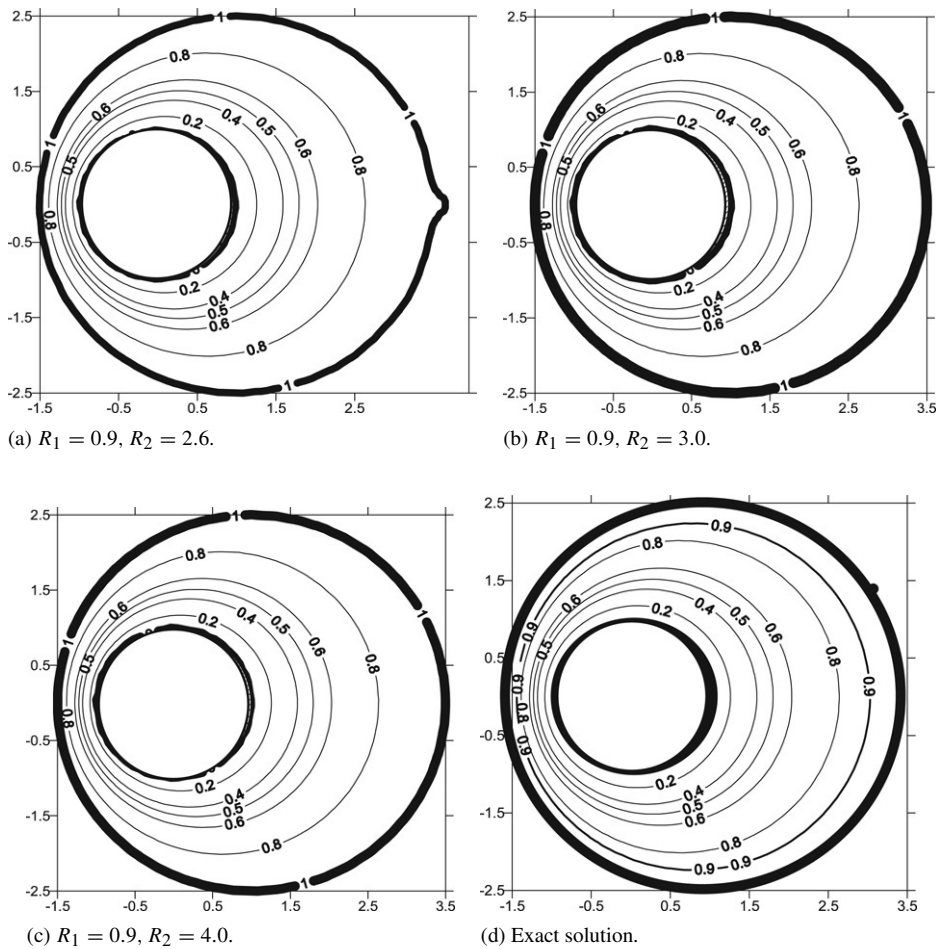
Fig. 11. Contour plots for the eccentric case using the MFS (inner: 20 points; outer: 60 points).

fictitious source depends on the number of nodes. Also the ill-conditioned behaviour appears when R is larger than 2.4 for $N = 35$. For clarity, the error of norm ($\dfrac{\int_\Omega [u(x) - u_e(x)]^2 dx}{\int_\Omega u_e^2(x) dx}$, where $u_e(x)$ is the exact solution) versus the number

(a) $N_T = 6$.

(b) $N_T = 14$.

(c) $N_T = 26$.

(d) Exact solution.
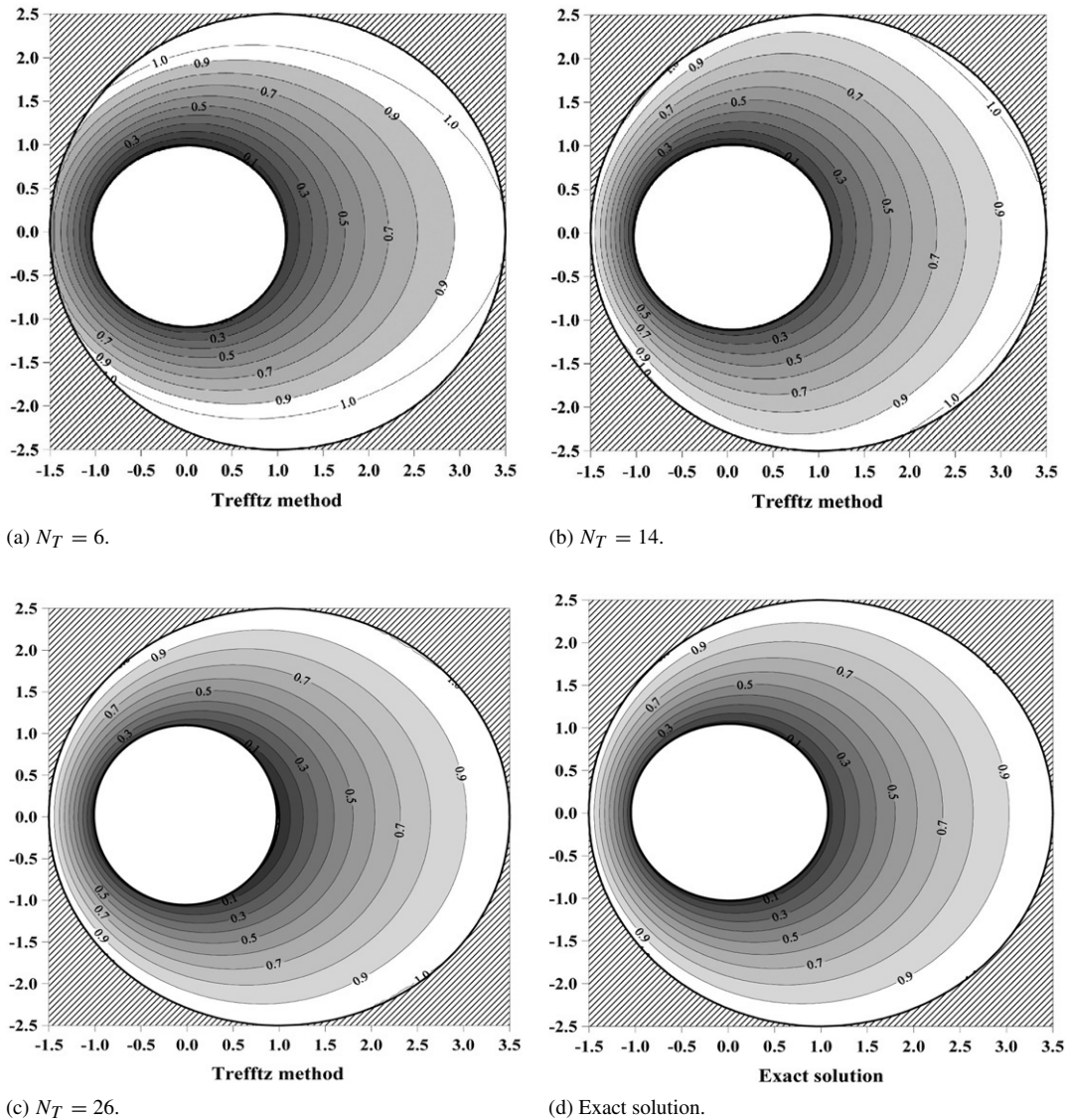
Fig. 12. Contour plots for the eccentric case using the Trefftz method.

of source points is shown in Fig. 15 for the example (Fig. 4(a)). For the larger number of d.o.f. ($N > 8$), the error for the potential prediction by using the Trefftz method is larger than that of MFS. In the range of $N < 8$, the conclusion is contrary. Based on the Figs. 14 and 15, this numerical experiment shows that the optimal value of R depends on the number of source points. However, an objective guideline for the optimal value of R is still a challenge to MFS. Until now, no objective criterion for the optimal position of sources has been proposed. It is found that the optimum location depends on the number of source points. This is the reason why a general rule can't be suggested. For the test case, we can't predict which one is better to calculate the normal gradient on the boundary. Since the Trefftz method can be seen as one kind of Fourier series solution as well as the MFS. For the test example, the boundary potential is not continuous at points $(1,0)$ and $(-1,0)$. The rate of convergence of the gradient is slower than that of the temperature itself, but both improve with decreasing ρ. It fails to calculate the gradient at the boundary. The result has been studied in references [16,17]. The error norms of x- and y- gradients for the domain are plotted in Fig. 16(a) and (b). It is worth mentioning that MFS can have different results for different values of R. It is found that the accuracy of MFS is better than that of the Trefftz method in solving the potential gradients under the same number of degree of freedoms based on the given case.
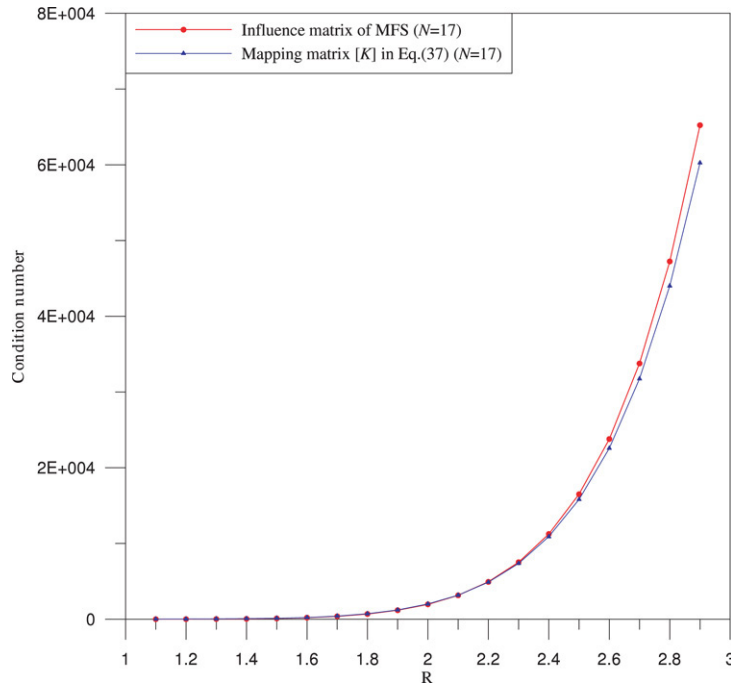
Fig. 13. The condition number of mapping matrix and influence matrix of MFS versus locations of distribution sources.
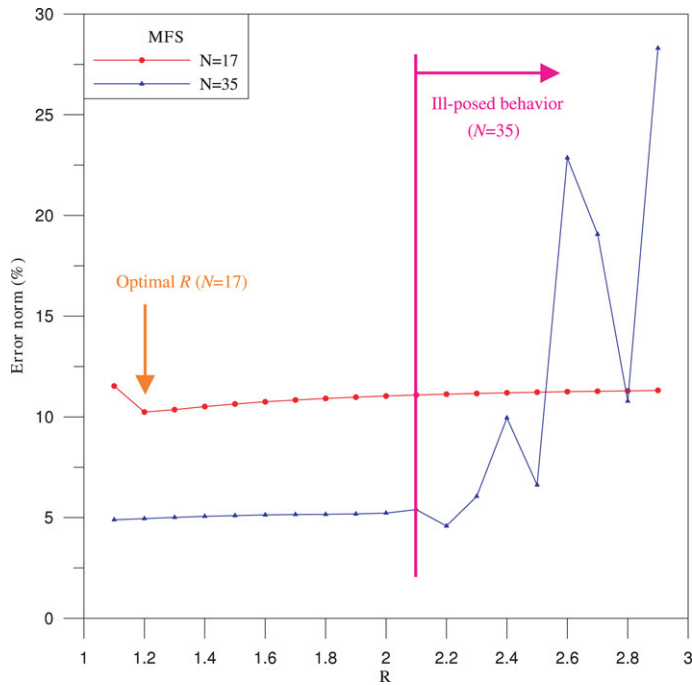
Fig. 14. Error norm versus R by using the method of fundamental solutions.

6. Conclusions

In this paper, the proof of the mathematical equivalence between the Treffz method and the MFS for both Laplace and biharmonic problems was derived. It is interesting to find that the complete set in the Trefftz method is imbedded
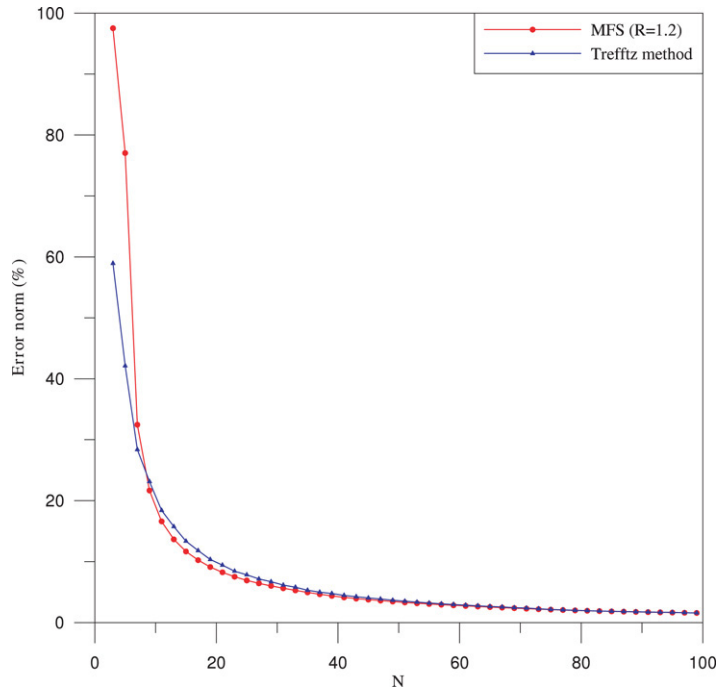
Fig. 15. Error norm versus the number of collocation points by using the Trefftz method and the method of fundamental solutions.
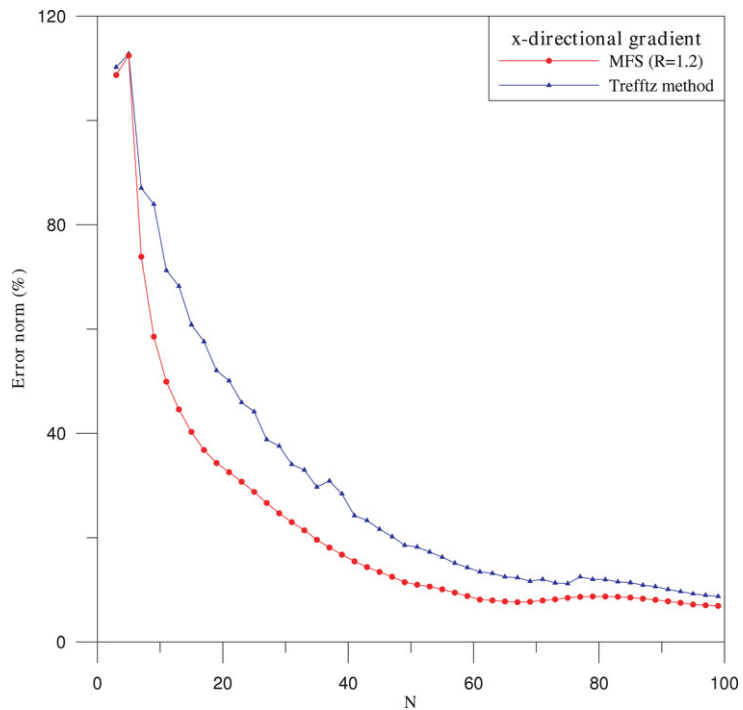
(a) *x*-gradient.

Fig. 16. Error norm of *x*- and *y*-gradients.
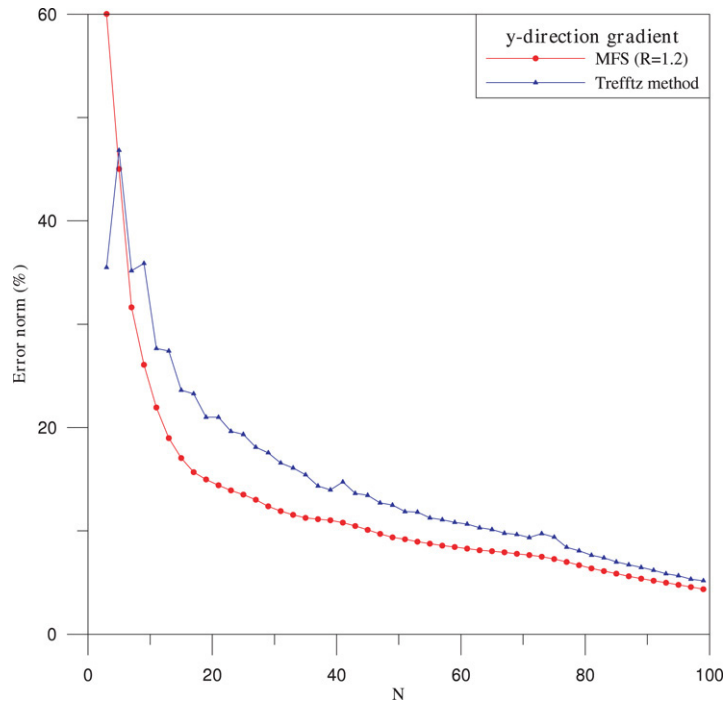
(b) *y*-gradient.

Fig. 16. (*continued*)

in the degenerate kernels of MFS for the interior and exterior problems of the Laplace and biharmonic equations. The degenerate scale occurs when using the MFS since the source points locate at the critical scale. The ill-posed problem in the MFS also stems from the geometrical matrix when the source is distributed far away from the real boundary. Both the Trefftz method and the MFS were employed to solve the interior and exterior Laplace problems with simply-connected and doubly-connected domains. The convergence and efficiency of the two methods were also discussed. For the degenerate scale problem, we have the nonuniqueness solution when the radius a approaches 1 ($\ln(a) = 0$) of the Laplace problem. For the biharmonic problem, the degenerate scale occurs when the fictitious sources are located at e^0, $e^{\frac{-1}{2}}$ and e^{-1} for the circular case. Based on the present study, we can avoid the occurrence of degenerate scale problem in the MFS by adjusting the fictitious boundary.

References

[1] K. Andreas, G. Fairweather, The method of fundamental solutions for axisymmetric potential problems, International Journal for Numerical Methods in Engineering 44 (1999) 1653–1669.

[2] J.R. Chang, R.F. Liu, W.C. Yieh, S.R. Kuo, Applications of the direct Trefftz boundary element method to the free-vibration problem of a membrane, Journal of the Acoustic Society of America 112 (2) (2002) 518–527.

[3] J.T. Chen, On the fictitious frequencies using dual series representation, Mechanics Research Communication 25 (1998) 529–534.

[4] J.T. Chen, J.H. Lin, S.R. Kuo, Y.P. Chiu, Analytical study and numerical experiments for degenerate scale problems in boundary element method using degenerate kernels and circulants, Engineering Analysis with Boundary Element 25 (9) (2001) 819–828.

[5] G. Fairweather, A. Karageorghis, The method of fundamental solutions for elliptic boundary value problems, Advances in Computational Mathematics 9 (1998) 69–95.

[6] W.G. Jin, Y.K. Cheung, O.C. Zienkiewicz, Application of the Trefftz method in plane elasticity problems, International Journal for Numerical Methods in Engineering 30 (1990) 1147–1161.

[7] W.G. Jin, Y.K. Cheung, O.C. Zienkiewicz, Trefftz method for Kirchhoff plate bending problems, International Journal for Numerical Methods in Engineering 36 (1993) 765–781.

[8] J. Jirousek, A. Wroblewski, *T*-elements: State of the art and future trends, Archives of Computational Methods in Engineering 3–4 (1996) 323–434.

[9] A. Karageorghis, G. Fairweather, The method of fundamental solutions for the numerical solution of the biharmonic equation, Journal of Computational Physics 69 (2) (1987) 434–459.

[10] A. Karageorghis, G. Fairweather, The Almansi method of fundamental solutions for solving biharmonic problems, International Journal for Numerical Methods in Engineering 26 (1988) 1665–1682.

[11] A. Karageorghis, G. Fairweather, The simple layer potential method of fundamental solutions for certain biharmonic problem, International Journal for Numerical Methods in Fluid 9 (1989) 1221–1234.

[12] A. Karageorghis, G. Fairweather, The method of fundamental solutions for axisymmetric potential problems, International Journal for Numerical Methods in Engineering 44 (1999) 1653–1669.

[13] E. Kita, N. Kamiya, Trefftz method: An overview, Advances in Engineering Software 24 (1995) 3–12.

[14] V.D. Kupradze, A method for the approximate solution of limiting problems in mathematical physics, Computational Mathematics and Mathematical Physics 4 (1964) 199–205.

[15] D. Polyzos, G. Dassios, D.E. Beskos, On the equivalence of dual reciprocity and particular integral approaches in the BEM, Boundary Element Communications 5 (1994) 285–288.

[16] J.T. Chen, M.T. Liang, S.S. Yang, Dual boundary integral equations for exterior problems, Engineering Analysis with Boundary Elements 16 (1995) 333–340.

[17] Test No. 2, Two dimensional steady state heat conduction with a circular boundary in an infinite domain, Boundary Elements Abstracts 1 (2) (1990) 90–91.